Polymer 53 (2012) 4211–4221

Contents lists available at SciVerse ScienceDirect

Polymer

journal homepage: www.elsevier.com/locate/polymer

Characterization of the oxygen scavenging capacity and kinetics of SBS films

Kevin K. Tung, R.T. Bonnecaze, B.D. Freeman, D.R. Paul*

Department of Chemical Engineering and Texas Materials Institute, The University of Texas at Austin, Austin, TX 78712, United States

ARTICLE INFO

Article history:
Received 21 June 2012
Received in revised form
6 July 2012
Accepted 14 July 2012
Available online 20 July 2012

Keywords:
Butadiene
Oxidation
Permeation

ABSTRACT

Butadiene-containing polymers such as styrene-butadiene-styrene (SBS) block copolymers are of a potential use as oxygen scavenging polymers (OSP) in barrier applications. To evaluate their use in such applications, oxygen uptake was measured for films made of an SBS copolymer and four cobalt catalyst loadings with various thicknesses. The oxygen uptake was found to be kinetically limited for thin films while diffusion controls the uptake at long times for thick films. The thickness of the oxidized region at long oxidation times is termed the critical thickness L_c and was quantified by various analyses. Thin films (i.e.,$L \leq 2L_c$) oxidize fully and homogeneously, whereas heterogeneous oxidation typically occurs in thicker films (i.e., $L > 2L_c$). A thin film model was used to extract the reaction rate parameters and a stoichiometric oxidation coefficient that describe oxygen uptake in the absence of diffusion limitation. An approximate moving-boundary model was developed to describe thick film oxidation behavior at long times and was found to be in semi-quantitation agreement with the measured uptake.

1. Introduction

Polymers are often favored as barrier materials because they are easily formed into films, sheets or bottles and are lighter in weight than alternatives like glass or metal [1]. However, for some foods and beverages, or even electronic components [2–4], there is a need for polymeric formulations that limit the ingression of oxygen into the contents of a package to a much greater extent than simple polymeric barrier materials can provide. An approach that has attracted interest in recent times is to include oxygen scavenging components into a polymeric film or bottle wall [5,6]; temporarily, this can greatly reduce the amount of oxygen reaching the package contents. This can be an effective strategy when the duration of this retarded oxygen influx is greater than the anticipated shelf life of the product. Implementation of this technique requires a judicious combination of experimental development of formulations, mathematical modeling and determination of model parameters by matching models to experiments; this has been a focus of recent research in this laboratory [7–14].

The concept envisioned requires one polymer chosen for its structural characteristics, which could also be a reasonably good barrier material like poly(ethylene terephthalate) by virtue of its low oxygen permeability, and an oxygen scavenging polymer, OSP, that chemically reacts with oxygen. The latter might be incorporated as a dispersed phase in a blend film [7,9] or layers in a multilayer film [13,14] made by coextrusion. Butadiene-containing polymers are attractive materials for oxygen scavenging since the carbon–carbon double bonds provide sites for significant oxygen reaction [15–20]; this rate can be regulated by the addition of certain catalysts [12,21,22].

The rate and extent of oxygen uptake by the scavenging component can be measured experimentally as described in numerous publications [10–12]. The extent of oxygen uptake in such experiments appears to plateau to an asymptotic value at times of the order of weeks or months [12]. The plateau value is essentially independent of film thickness when below a certain "critical thickness", but for thicker films the plateau value decreases with increasing thickness [23–25]. This is a complex process involving the physical dissolution of oxygen into the polymer, oxygen diffusing through the polymer, and reaction of the polymer with oxygen [26,27] with physical parameters being significantly affected by the chemical state of the OSP. There is ample evidence that the oxidation process is spatially heterogeneous involving a moving front in thick films [9–12,23–25]. The apparent plateau in oxygen uptake for thick films does not really mark a true end-point of the process but simply a greatly reduced rate of uptake limited by a much lower rate of diffusion through the oxidized layer owing to the changes in the intrinsic transport characteristics of the polymer resulting from the formation of polar structures by the oxidation reactions and, of course, the growing thickness of this region.

Prior analyses of the oxygen uptake by the scavenging polymer [12,28] have not adequately reduced the results to fundamental

* Corresponding author. Tel.: +1 512 471 5392; fax: +1 512 471 0542.
E-mail address: drp@che.utexas.edu (D.R. Paul).

0032-3861/$ – see front matter © 2012 Elsevier Ltd. All rights reserved.
http://dx.doi.org/10.1016/j.polymer.2012.07.028

parameters that can subsequently be used to model the oxygen flux emerging from a blend or layered film during its functional life time, i.e., prior to the eventual breakthrough of oxygen when all the OSP has reached its scavenging capacity [7–9,13,14]. The purpose of this paper is to explore the oxygen uptake by an attractive oxygen scavenging system, viz., a styrene-butadiene-styrene, SBS, block copolymer containing varying amounts of a cobalt catalyst, for a wide range of film thicknesses. It will be shown that for thin enough films, the rate of oxygen uptake is not limited by diffusion and the results can be analyzed by a simple chemical kinetic model to obtain stoichiometric and reaction rate parameters. For thicker films, oxygen diffusion becomes limiting and the results can be understood semi-quantitatively in terms of a moving-boundary model. The "critical thickness" dividing the two regimes deduced from long term oxygen uptake data agrees well with post-mortem microscopic inspection of the partially oxidized film. The parameters deduced here should be useful for future design and modeling of blend and laminate barrier films based on this SBS/cobalt catalyst system.

2. Experimental

2.1. Materials

Styrene-butadiene-styrene block copolymers are a more convenient oxygen scavenging polymer than polybutadiene used in previous studies [10–12] owing to ease of handling and processing plus their potential compatibility, i.e., interfacial tension and adhesion, with the selected structural polymer. The SBS used here is a commercial product of Kraton Polymers, Inc., D1102, containing 28 wt.% styrene and 72 wt.% butadiene, of which 92 wt.% is 1,4 polybutadiene, with an overall $M_n = 100{,}000$.

Benzophenone (>99%), used as a photoinitator to produce radicals that triggers oxidation given a proper source of UV energy [15,17,19,28–32], was purchased from Sigma–Aldrich and used as received. The oxidation catalyst [12,33] was purchased from Shepherd Chemical Company (Cincinnati, OH) in the form of blue solid pastilles that contains 20.5 wt.% cobalt neodecanoate. The cobalt catalyst was diluted 100 times (by volume), using cyclohexane, in a volumetric flask. Cyclohexane (99.9%) was purchased from Fisher Chemical and used as received. Silicon wafers (5-in and 2-in diameter) were purchased from Addison Engineering Inc. (San Jose, CA).

2.2. Film preparation

Reactive films were made by both solution casting and spin coating techniques [11]. In solution casting, the polymer was dissolved in cyclohexane to make a 2 wt.% solution in an amber glass bottle. Predetermined amounts of cobalt neodecanoate solution and benzophenone were added to the stirred solution. After the additives were fully dissolved, the homogeneous solution was poured into a glass ring (5.1 cm in diameter) resting on a glass plate. The nacent film on the glass plate was held under nitrogen in a glove box covered with aluminum foil to allow the cyclohexane to slowly evaporate. The resulting films were stored in a vacuum oven at room temperature for an additional 6 h to fully remove the solvent. Film thicknesses were determined using a Mitutoyo Litematic VL-50A instrument (Mitutoyo Corporation, Japan) specially designed to measure the thickness of rubbery films. In this study, solution casting was used to form films with thicknesses ranging from 50 to 250 μm.

In spin coating, SBS solutions were filtered through a 5.0 and 0.2 mm Whatman® PURADISC™ Teflon syringe filter before use. From the filtered SBS solution, thin films were spin coated onto a clean, polished, native-oxide silicon (100) wafer using a Laurel WS–400B–8NPP/LITE model spin coater (North Wales, PA) at 1000 rpm for 60 s. In this study, spin coating was used to form films with thicknesses ranging from 1 to 15 μm. For oxygen mass uptake experiments, these films were left on the silicon wafers to oxidize. Since silicon wafers are impermeable to gases, the SBS films were oxidized from only one surface.

To prepare film samples for permeation experiments, 3 cm × 3 cm pieces of the thin films were cut with a razor blade and then detached from the wafer surface by immersing the wafer-film composite in deionized water. A thin wire frame described earlier [12] was used to transfer the films into a vacuum oven, where they were dried at room temperature for 1 h before use.

While the thin films were on the silicon wafer, their thicknesses were determined using a KLA-Tencor Instrument Alpha-step 200 profilometer (Mulpitas, CA). First, a small nick was cut on films using a razor blade. Physical contact of the profilometer tip with the film and the wafer gives a measure of the nick depth or the thickness of the spin-coated film.

2.3. Oxygen uptake measurement

A UV light source providing a predetermined amount of energy was used to irradiate the SBS films containing benzophenone as a photoinitator to initiate oxidation. The overall UV energy provided is a function of UV light intensity, film distance from the light source, and exposure time. To prevent premature oxidation, polymer films were kept free of oxygen by storing under an inert atmosphere (nitrogen) until the oxygen uptake experiments began. The irradiated films were kept in a temperature controlled chamber at 35 °C for the duration of the oxidation experiment. Oxygen mass uptake was tracked by monitoring weight changes of the films on a Mettler Toledo AB54-S/FACT analytical balance (accuracy to 0.1 mg); oxygen uptake is taken as the difference between the film mass at any given time and its initial mass before the start of sorption experiments. Film samples were oxidized in ambient air, ~21% oxygen, as a function of time.

The oxidation of butadiene units under the conditions of interest here involves rather complex chemistry, and the details of the reaction are beyond the scope and the interests of the current study. The butadiene units can be imagined as reactive sites that consume oxygen [10,11,17]. Since SBS D1102 has a density of 0.94 g/cm^3 and contains 72 wt.% butadiene, the concentration of butadiene units is approximately 12.2 $mmol_{PB}/cm^3$. For subsequent analysis, the initial concentration of unreacted butadiene units will be designated as n_0 and a stoichiometric coefficient $\hat{\nu}$ defines the ratio of moles of butadiene units that reacts with each mole of O_2 and will be determined experimentally. In order to make the reaction rates fast enough for practical use in barrier systems, the cobalt catalyst mentioned must be added.

2.4. Gas transport properties measurement

The permeability of SBS films to nitrogen and oxygen was measured using a constant volume/variable pressure apparatus [34]. Because conventional packaging is usually designed to minimize oxygen permeance, oxygen is a gas of direct interest in characterizing these new oxygen scavenging materials. Nitrogen is an inert, non-oxidizable gas molecule similar in size to oxygen that can be used to determine and confirm changes in gas transport properties in samples without furthering oxidation.

Solution cast thick films were masked, with openings on their upstream and downstream sides, using impermeable aluminum tape. Spin-coated thin films mounted on the copper wire frame were carefully placed at the center of a Whatman Anodisc® for

mechanical support [12]. Aluminum tape with center openings to permit gas permeation was then applied to both sides. The gas permeability P was calculated from (1):

$$P = \frac{V \cdot l}{p_1 \cdot A \cdot R \cdot T}\left[\left(\frac{dp_2}{dt}\right)_{ss} - \left(\frac{dp_2}{dt}\right)_{leak}\right] \quad (1)$$

where p_1 is the upstream absolute pressure, T is absolute temperature, A is the film area, l is the film thickness, V is the downstream volume, R is the gas constant, and $(dp_2/dt)_{ss}$ and $(dp_2/dt)_{leak}$ are the pseudo-steady state rates of pressure rise in the downstream volume at a fixed upstream pressure and under vacuum, respectively. A downstream pressure less than 10 torr was maintained during all measurements.

The nitrogen and oxygen permeability coefficients of both un-oxidized (~350 μm) and fully oxidized (~3.7 μm) polymers were determined from the slopes of the linear, steady-state region of curves of increasing downstream permeate pressure versus time. Moreover, the intercept of the steady-state line on the time axis, or the time lag, θ, was used to calculate the diffusion coefficient for the un-oxidized polymer [34].

$$D = L^2/6\theta \quad (2)$$

The dual-volume pressure-decay method was used to determine gas solubility coefficients of fully oxidized polymer [34]. The sample cell, that contains fully oxidized polymer, is first evacuated and isolated from the charge cell, which is charged with an experimental gas at a pressure of interest. Then the valve connecting the sample and charge cells was opened to allow pressure stabilization, which is monitored as a function of time. Initial and final pressure values in the sample and charge cells were used to calculate the concentration of gas sorbed in the fully oxidized polymer at a specific pressure value. Subsequently the sorption isotherms were constructed by relating concentration of gas sorbed in the sample for several pressures. Then the sorption coefficient was calculated from,

$$S = C/p \quad (3)$$

The permeability is given by the product of diffusion and sorption coefficients [34],

$$P = D \times S \quad (4)$$

By Equation (4) gas solubility coefficients of un-oxidized polymer were calculated using the known values of gas permeability and diffusion coefficients. Similarly, the ratio of gas permeability and solubility coefficient of a fully oxidized polymer gives its diffusion coefficient.

2.5. Scanning electron microscopy (SEM)/energy dispersive spectroscopy (EDS)

Samples of thick films that had been oxidized for ~90 days were used to expose a surface perpendicular to the plane of the film for SEM analysis by first cutting with a glass knife and then with a diamond knife (Micro Star Technologies, Huntsville, TX) using an RMC-Boeckeler PowerTome PT-XL (Boeckeler Instruments Inc., Tucson, AZ) at cryogenic temperature (−125 °C) at a cutting speed of 0.8 mm/s. The resulting SEM samples were secured with carbon tape perpendicularly on low profile 45°/90° SEM mounts (Ted Pella Inc., Redding, CA) and then coated with a 10 nm layer of indium using an Emitech K575K sputter coater (Quorum Technologies Ltd., West Sussex, United Kingdom) operated 150 μW for 10 s and viewed using a Zeiss NEON 40 FE-SEM (Carl Zeiss SMT Inc., Peabody, MA) operated at 5 kV and ~20 mm working distance. The SEM images were made immediately to limit further oxidation of the microtomed surfaces.

Partially oxidized films were immersed into liquid nitrogen and fractured to create a cross-sectional surface. The resulting samples were then immediately secured with carbon tape on an SEM mount with no metal coating. Afterward, energy dispersive x-ray spectroscopy (detector = Bruker EDS Quantax 4010) was used for elemental analysis on partially oxidized films to examine the presence of oxygen-containing functional groups throughout the film thickness, by means of stoichiometric ratios, multiple elemental line scanning, and 2-dimensional mapping.

2.6. Polymer density measurement

Polymer density was characterized using the Archimedes principle, which gives

$$\rho_p = \frac{M_A}{M_A - M_L}\rho_0 \quad (5)$$

where ρ_p and ρ_0 are the densities of the target polymer and the auxiliary liquid used, respectively, while M_A and M_L are the film mass in air and in the auxiliary liquid, respectively. Film density was determined using a Mettler Toledo AB54-S/FACT analytical balance (accuracy to 0.1 mg) and a density kit. Hexane (0.655 g/cc, Fisher Scientific) was used as the auxiliary liquid.

3. Results and discussions

3.1. Gas sorption and permeation

The gas transport properties of un-oxidized and fully oxidized SBS films were characterized and are recorded in Table 1. Nitrogen and oxygen transient permeation experiments were conducted with a ~350 μm un-oxidized film at 35 °C. The nitrogen and oxygen permeability coefficients were determined from the steady-state region while the time lag was used to calculate the nitrogen and oxygen diffusion coefficients. The solubility coefficients shown were calculated from the ratio of the permeability and diffusion coefficient of the un-oxidized polymer. Gas transport properties of commercial SBS D1102 are reasonably close to those of other SBS materials reported in the literature [12,35–38].

A 3.7 μm reactive film containing 800 ppm cobalt catalyst was exposed to an upstream oxygen pressure of 7 atm for rapid oxidation over 4–6 h at 35 °C in a gas permeation cell. The gas permeability dropped quickly with time, and the final stabilized nitrogen and oxygen permeability coefficients shown in Table 1 were determined. For the gas solubility coefficients, the fully oxidized sample was first placed in a sorption cell and allowed to absorb nitrogen at various pressures up to 7 bar at 35 °C. This dual-volume pressure-decay method [34] uses initial and final pressure values in the sample and charge cells to calculate the concentration of gas sorbed per unit volume of fully oxidized polymer at a specific pressure.

A nitrogen sorption isotherm at 35 °C was first constructed, followed by an oxygen sorption isotherm. Afterward a second nitrogen sorption isotherm was produced and found to be similar to the first nitrogen sorption isotherm. This exercise ensures data reproducibility and confirms the sample of interest is indeed full oxidized. The concentration of nitrogen and oxygen sorbed in the fully oxidized sample was found to vary linearly with gas pressure. The values of nitrogen and oxygen solubility coefficients of fully oxidized polymer were determined and are shown in Table 1, which also shows values of diffusion coefficients that were calculated as

Table 1
Gas transport properties of SBS, 1,4 PB, and PS.

	$P\ 10^{-10}\frac{cm^3(STP)\cdot cm}{cm^2\cdot s\cdot cm\ Hg}$		$S\ 10^{-4}\frac{cc(STP)}{cm^3\cdot cm\ Hg}$		$D\ 10^{-6}\frac{cm^2}{s}$		ρ g/cm^3
Sample/gas	N_2	O_2	N_2	O_2	N_2	O_2	
SBS D1102[a]	22	56	4.5	9.1	4.6	6.0	0.94
SBS D1102[a] (Fully oxidized)	0.18	0.41	13	16	0.01	0.03	1.2
SBS [35]	9.7	23.9	6.9	9.9	2.4	1.4	–
SBS [36]	14	40	–	–	–	–	–
SBS D1101 [38]	–	26.1	–	–	–	–	–
SBS D1107 [38]	–	19.0	–	–	–	–	–
1,4 PB [12]	10.3	24.3	–	–	–	–	–
1,4 PB [12] (Fully oxidized)	0.04	0.14	–	–	–	–	–
cis-1,4 PB [37]	6.5	19.1	5.9	13	1.1	1.5	–
PS[a]	0.50	3.1	8.9	23	0.06	0.14	1.06
PS [36]	0.22	1.2	–	–	–	–	–
PS [38]	0.24–0.30	1.8–2.4	–	–	–	–	–

[a] This work.

the ratio of permeability and solubility coefficients of fully oxidized polymer.

Oxidation reduced the gas permeability coefficients of the SBS films by approximately 2 orders of magnitude, which is comparable to that observed earlier for reactive films of 1,4 polybutadiene [12]. This level of change in gas permeability is due to the reduction in the gas diffusion coefficients as the butadiene segments are converted to more polar oxygen containing units and perhaps to crosslinking [12]. In general, addition of oxygen-containing functional groups are expected to reduce the polymer free volume [37,39,40]. On the other hand, gas solubility coefficients were found to increase slightly by a factor of two to three. This is reasonable since oxidized SBS rubber essentially becomes a glassy polymer, similar to that observed in earlier work on 1,4 polybutadiene oxidation [12]. Typically, glassy polymers sorb greater quantities of gas than do rubbery polymers [41].

3.2. Oxygen uptake: critical thickness

A set of reactive SBS films, with catalyst loadings of 100, 200, 400, 800 ppm, were cast with a wide range of thicknesses from 1 to 300 μm and were allowed to oxidize for approximately 90 days at 35 °C. The oxygen uptake M_t observed at any time t was normalized by the polymer mass prior to any oxidation. Fig. 1(a) shows an example of oxygen uptake versus time curves at 200 ppm catalyst loading for a range of thicknesses from 2.8 to 266 μm. Other catalyst loadings yield similar, but quantitatively different, responses.

The thinner films, <14 μm, represented by the solid points in Fig. 1(a) appear to fall on the same uptake curve that is independent of film thickness. This suggests that these thinner films oxidize uniformly throughout their thickness and eventually reach a constant extent of oxidation. This constant uptake value at long oxidation times for the 200 ppm catalyst loading samples, 26.6 ± 1.0 gram of oxygen/100 gram of polymer, can be considered as the oxygen uptake that can be achieved when given an infinite amount of time, M_∞. This value is the same for all thin films of each catalyst loading within experimental error; values of M_∞ obtained at all catalyst loadings for thin film samples are recorded in Table 2.

The thicker films, >58 μm, have similar oxidation kinetics as the thinner films at early oxidation times, where the oxygen uptake increases rapidly with time. However, the oxygen uptake at long oxidation times is found to be a function of film thicknesses, i.e., the uptake, normalized by the original polymer mass, at any time decreases with increasing film thicknesses. Moreover, the rate of oxygen uptake was found to decrease with time as can be seen by comparing the respective slopes in the early and long time regimes, as illustrated in Fig. 1(b) for 117 and 232 μm thick films using log–log coordinates. At short times, the uptake appears to increase linearly in time but this gives way at much longer times to a slower regime where M_t appears to be approaching an increase

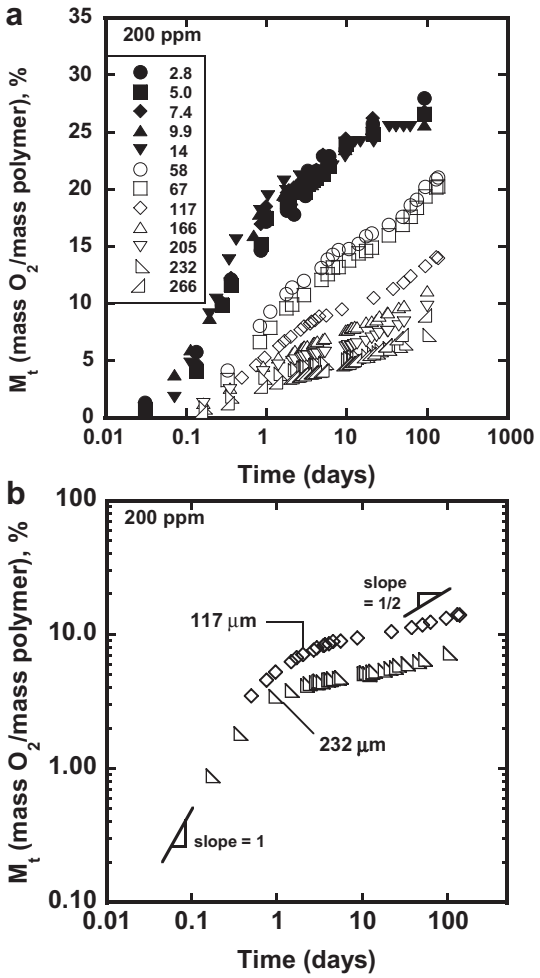

Fig. 1. Effect of thickness (2.8–266 μm) on oxygen uptake for SBS films containing 200 ppm catalyst: (a) Data for thin films (solid points) collapse into a single curve that eventually reaches a constant extent of oxidation, while for thick films (open points) uptake strongly depends on thicknesses. (b) A plot using log–log coordinates suggests that early time uptake varies as t while at longer times a $\sqrt{t}$ regime is approached.

Table 2
Kinetics parameters from thin film analysis; critical thicknesses ~90 days.

Parameter	Units	Catalyst loading, ppm			
		100	200	400	800
M_∞	$\frac{\text{gram of oxygen}}{\text{100 gram of polymer}}$	26.7 ± 1.1	26.6 ± 1.0	24.9 ± 1.7	21.9 ± 1.0
$\hat{\nu}$	$\frac{\text{mol}_{PB}}{\text{mol}_{O_2}}$	1.54 ± 0.06	1.56 ± 0.06	1.67 ± 0.11	1.88 ± 0.12
$1/\hat{\nu}$	$\frac{\text{mol}_{O_2}}{\text{mol}_{PB}}$	0.65 ± 0.03	0.64 ± 0.03	0.60 ± 0.04	0.53 ± 0.03
k_R	$\frac{\text{cm}^3}{\text{mol}_{PB}\cdot\text{sec}}$	7.9 ± 0.5	17.1 ± 2.4	25.3 ± 4.2	48.3 ± 6.0
L_c (1/L)	μm	31.1 ± 0.1	33.8 ± 0.1	40.8 ± 0.4	35.1 ± 0.2
L_c (SEM)	μ	30.0 ± 2.0	32.0 ± 2.0	38.0 ± 2.0	35.0 ± 2.0

proportional to $t^{1/2}$ suggestive of a diffusion controlled regime as developed later.

The implication of the M_t dependence on film thickness is that the thinner films are fully oxidized at long times on the order of 90 days whereas the thicker films are only partially so and are continuing to oxidize. There is considerable evidence that for thick films oxidation is heterogeneous with an outer oxidized layer that slowly moves inward. It has been suggested that observations like these can be interpreted in terms of a critical thickness, L_c. In other words, homogeneous oxidation is possible for film thicknesses $L \leq 2L_c$ and heterogeneous oxidation when $L > 2L_c$, as illustrated in Fig. 2.

Fig. 3 shows oxygen uptake at ~90 days for reactive films containing 100, 200, 400, and 800 ppm catalyst loadings plotted against inverse film thicknesses, as suggested previously [12,23]. In the homogeneous oxidation region where $L \leq 2L_c$ oxygen uptake forms a horizontal line independent of thickness at an average value we designate as M_∞. In the heterogeneous oxidation region where $L > 2L_c$ oxygen uptake M_t increases, $t \cong 90$ days, with decreasing film thicknesses and takes the form of $M_t 0 \propto = \propto \propto 1/L$. The intersection of these two lines yields a thickness $L = 2L_c$ which divides the homogeneous and heterogeneous regimes of oxidation. The values of L_c for the various catalyst loadings at ~90 days of oxidation estimated by this analysis are recorded in Table 2.

Based on the ideas outlined above, we expect the ultimate uptake of oxygen M_∞ to be approximately the same for all films regardless of thickness. For thin enough films, this limit is reached within the time scale of these oxidation observations; whereas, for very thick films, it is presumed that reaching this limit would require longer times than for these observations, i.e., 90 days.

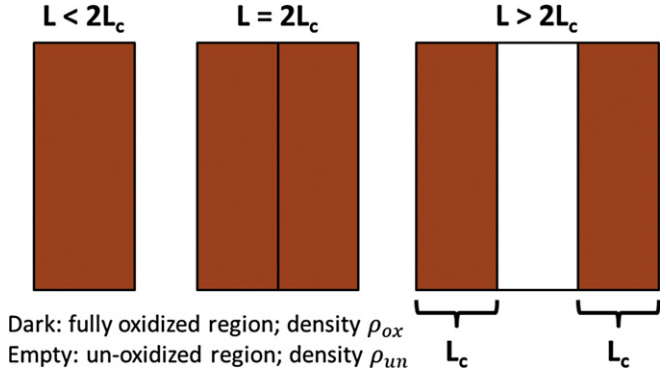

Fig. 2. Illustration of the concept of critical thickness. Homogeneous oxidation is possible for film thicknesses $L \leq 2L_c$ while heterogeneous oxidation occurs when $L > 2L_c$.

The quantity M_∞ can be expressed in terms of the molar density of butadiene repeating units available for oxidation $n_0 = 12.2$ mmol$_{PB}$/cm^3 for the current SBS copolymer, the stoichiometric oxidation coefficient $\hat{\nu}$ that describes how many moles of butadiene repeating units oxidized per mole of oxygen molecules, and the density of un-oxidized polymer, ρ_{un} as follows:

$$M_\infty = 32 n_0 / \rho_{un} \hat{\nu} \quad (6)$$

Table 2 shows values of $\hat{\nu}$ calculated from the M_∞ for thin films, i.e., $L \leq 2L_c$, that were fully oxidized at 90 days, see Fig. 3. These $\hat{\nu}$ values indicate that each butadiene unit takes up 1.1–1.3 oxygen atoms on average over the range of catalyst loadings used here.

With the view that ultimately the oxygen uptake of all reactive films would approach M_∞ at long enough time, it is then reasonable in the kinetic analyses discussed later to express oxygen uptake data as normalized values, i.e., M_t/M_∞.

3.3. SEM/EDS observations

It has been shown in earlier work that an un-oxidized film of 1,4 polybutadiene reveals a flat and smooth surface when microtomed [12]. In the current work, the SEM images were collected for SBS films oxidized for 90 days based on catalyst loadings of 100, 200, 400, and 800 ppm at 35 °C in air. Fig. 4(a) shows an SEM image of a microtomed cross-sectional surface of a partially oxidized film containing 200 ppm of catalyst. Here, the outer region is brittle and forms a scalloped fracture pattern when cut by microtoming. This can be attributed to oxidation forming a brittle, glassy polymer region. On the other hand, the inner region remains similar to that seen in the un-oxidized SBS and 1,4 polybutadiene [12] samples.

An EDS analysis, as shown in Fig. 4(b), clearly shows a high concentration of oxygen-containing functional groups in the outer surface layer in a cross-section of a film of SBS (200 ppm of catalyst), fractured by liquid nitrogen, that was oxidized for 5 days. This supportive illustration confirms that the brittleness found in the outer region of an oxidized film cross-section is primarily due to an oxidation front that progressively moves inward with time. Evidently a surface layer concentrated with oxidation by-products separates the inner regions that remain largely un-oxidized in a butadiene-containing reactive film [10–12]. The formation of such oxidized layers is the result of heterogeneous oxidation, i.e., a diffusion-controlled reaction, as in previous work on 1,4 polybutadiene reactive films [12]. The SEM image of a 200 ppm sample cross-section suggests a critical thickness, when oxidized for 90 days, observed at 32 ± 2.0 μm, which, along with values of

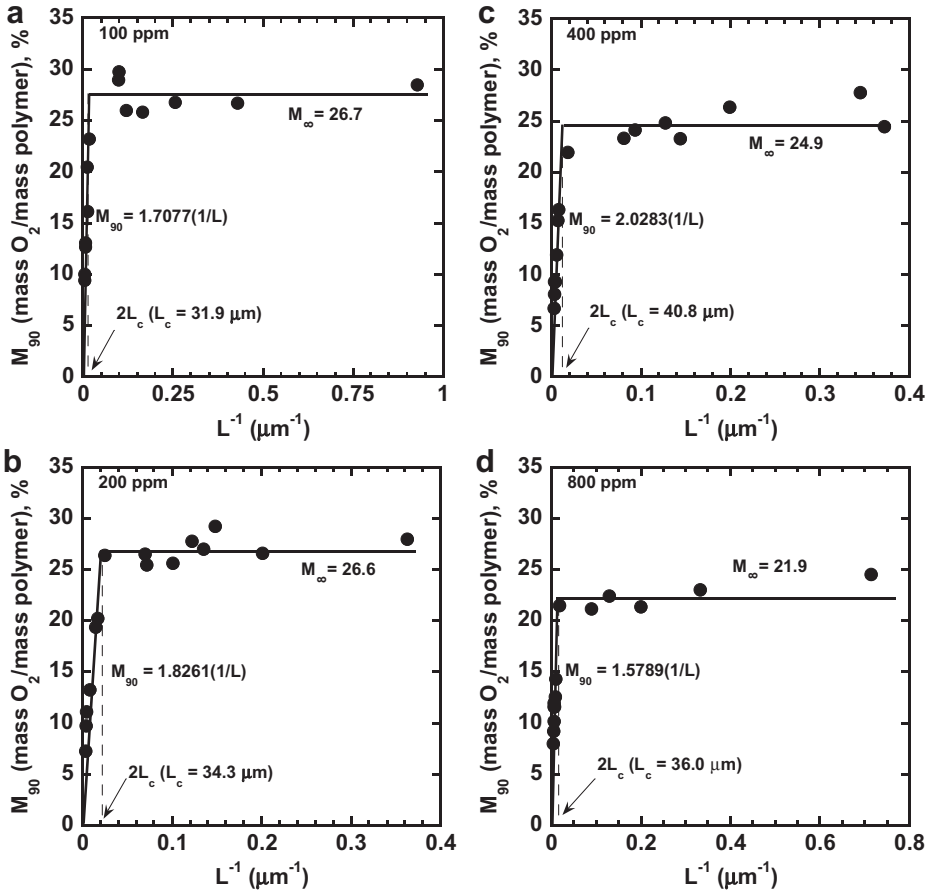

Fig. 3. Oxygen uptake at ~90 days for reactive films containing (a) 100, (b) 200, (c) 400, and (d) 800 ppm cobalt catalyst loadings plotted against inverse film thicknesses. For $L \leq 2L_c$, $M_{90} \sim M_\infty$, while for $L > 2L_c$, M_{90} varies as $1/L$.

samples of other catalyst loadings, are recorded in Table 2. These SEM-observed critical thicknesses and those determined by the inverse thickness analysis at 90 days agree very well, within experimental error, as illustrated in Fig. 5.

3.4. Kinetic analysis of thin films

Based on the discussion above it is reasonable to expect for thin enough OSP films (certainly less than L_c) that diffusion of oxygen is much faster than the reaction kinetics. In this limit of rapid oxygen diffusion, the concentration of dissolved oxygen in the film C is uniform throughout the thickness and would not vary with time; this oxygen concentration designated here as C_0 can be determined from the solubility of oxygen in the un-oxidized film at least in the early stages of the uptake experiment. On the other hand, the number of un-oxidized butadiene units, n, would be a function of time, starting from n_0 at $t = 0$, but would not be a function of position in the film. This scenario is schematically illustrated in Fig. 6.

The following simple kinetic model should describe the uptake processes assuming the reaction can be approximated as first order

$$\frac{\partial n(t)}{\partial t} = -\widehat{\nu} k_R C n(t) = -\widehat{\nu} k_R C_0 n(t) \tag{7}$$

where k_R is the first order reaction rate parameter. Using the initial conditions that $n = n_0$ at $t = 0$, the model solution becomes

$$n = n_0 e^{-\widehat{\nu} k_R C_0 t} \tag{8}$$

The mass of oxygen uptake, based on original polymer mass, is thus given by

$$M_t = \frac{32}{\rho_{\mathrm{un}} \widehat{\nu}} (n_0 - n) \tag{9}$$

Using Equation (6) for M_∞, the desired result becomes

$$\frac{M_t}{M_\infty} = \frac{n_0 - n}{n} = 1 - e^{-\widehat{\nu} k_R C_0 t} = 1 - e^{-t/t_{ox}} \tag{10}$$

where $t_{ox} = \widehat{\nu} k_R C_0$ defines a time scale for the oxidation process. For short enough times, a simple series expansion of the exponential term leads to

$$\frac{M_t}{M_\infty} = \widehat{\nu} k_R C_0 t \tag{11}$$

From the oxygen solubility coefficient for the un-oxidized SBS given in Table 1 and the partial pressure of oxygen in air, we obtain $C_0 = 6.71 \cdot 10^{-7}$ mol O_2/cm^3.

Fig. 7 shows the oxygen uptake data, normalized by the individual M_∞ for each film (not the average M_∞), plotted on log–log coordinates versus time for thin reactive films containing various catalyst loadings. The fractional oxygen uptake increases linearly with time and eventually reaches unity at times long enough for full oxidation. The rapid oxidation at early times can be modeled by Equation (11). Knowing $\widehat{\nu}$ and C_0, the reaction rate constant k_R for each film can be extracted from the data; the results are recorded in

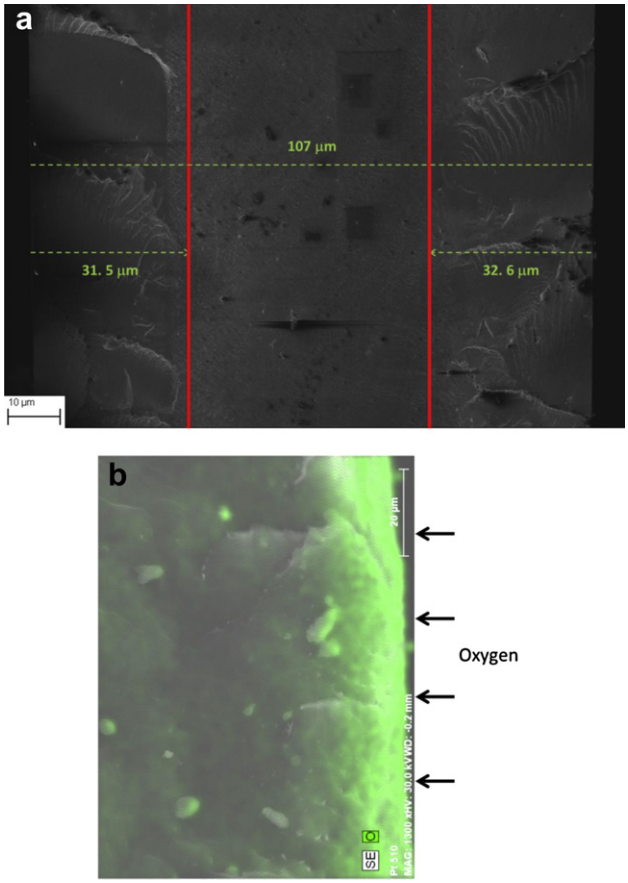

Fig. 4. An SEM image of a microtomed cross-sectional surface from an oxidized SBS film containing 200 ppm cobalt catalyst reveals outer oxidized layers with a thickness approximately 32.0 ± 2.0 μm at ~90 days. EDS image analysis clearly shows an accumulation of oxygen-containing functional groups at the outer surfaces of an SBS film (200 ppm of catalyst) that was oxidized for 5 days.

Table 2. These reaction rate constants increase monotonically with catalyst loading, within experimental error, as shown in Fig. 8.

The dotted lines in Fig. 7 represents the model prediction, Equation (10), of M_t/M_∞ calculated from the average k_R at each catalyst loading, see Table 2. The model results agree very well with the experimental M_t/M_∞ data over most of the oxidation process, as

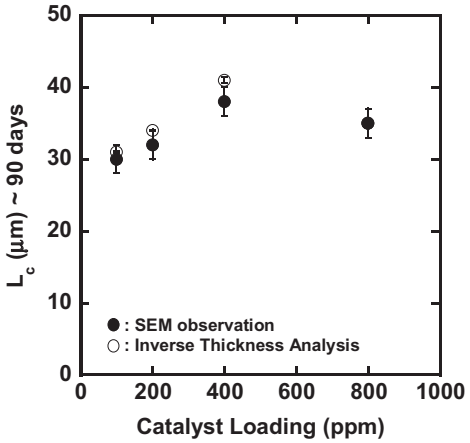

Fig. 5. The critical thicknesses at ~90 days evaluated by two separate analyses, SEM and oxygen uptake experiment, agree with each other within experimental error.

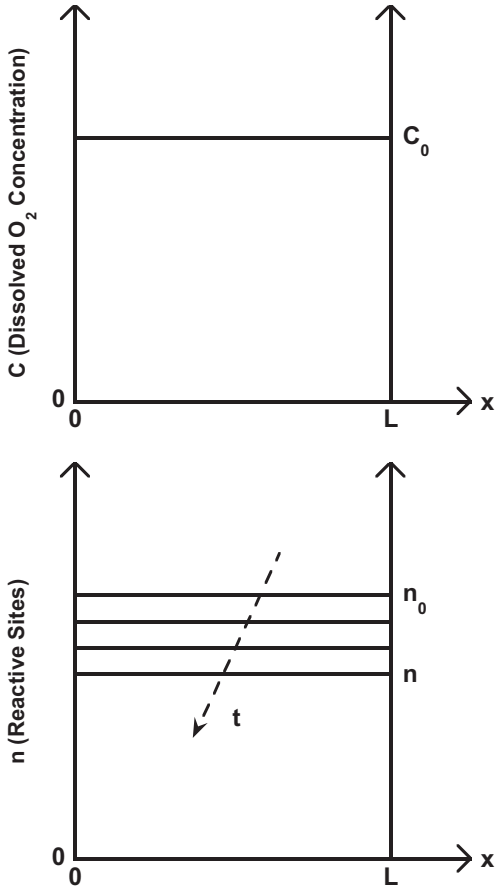

Fig. 6. Situation when oxidation is controlled by reaction kinetics because oxygen diffusion is relatively more rapid.

shown in Fig. 7; however, at long oxidation times, typically more than 1 day into oxidation, the model begins to over-predict the experimental M_t/M_∞ values. This probably reflects some level of diffusion control and a breakdown of the assumptions of the model.

3.5. An approximate model for thick films

In the very earliest stages of oxygen uptake in thick films, $L > 2L_c$, a regime like that described above should exist where diffusion is not limiting, as suggested in Fig. 3. However, as time progresses, diffusion should become more and more important until diffusion is the rate controlling process. Models that describe this progression, at least conceptually, have been proposed [7–9,13,14]. However, here we develop a simpler approach to illustrate the final stages of this uptake process.

Fig. 9 illustrates the physical basis of the proposed model. It envisions sharp oxidation fronts at x_f and $L-x_f$ moving inward from the two faces of the film. In the two outer layers of thickness x_f, all the butadiene units have been completely reacted up so $n = 0$ whereas in the core none of the butadiene units have yet reacted so $n = n_0$. The core shrinks in time as oxygen diffuses through the already oxidized outer layers at a pseudo-steady rate (for both faces of the film) given by

$$\text{Molar } O_2 \text{ flux} = \frac{D_{ox}C_0}{x_f} \tag{12}$$

where D_{ox} is diffusion coefficient of oxygen in the oxidized polymer and C_0 is the dissolved oxygen concentration at the external surface

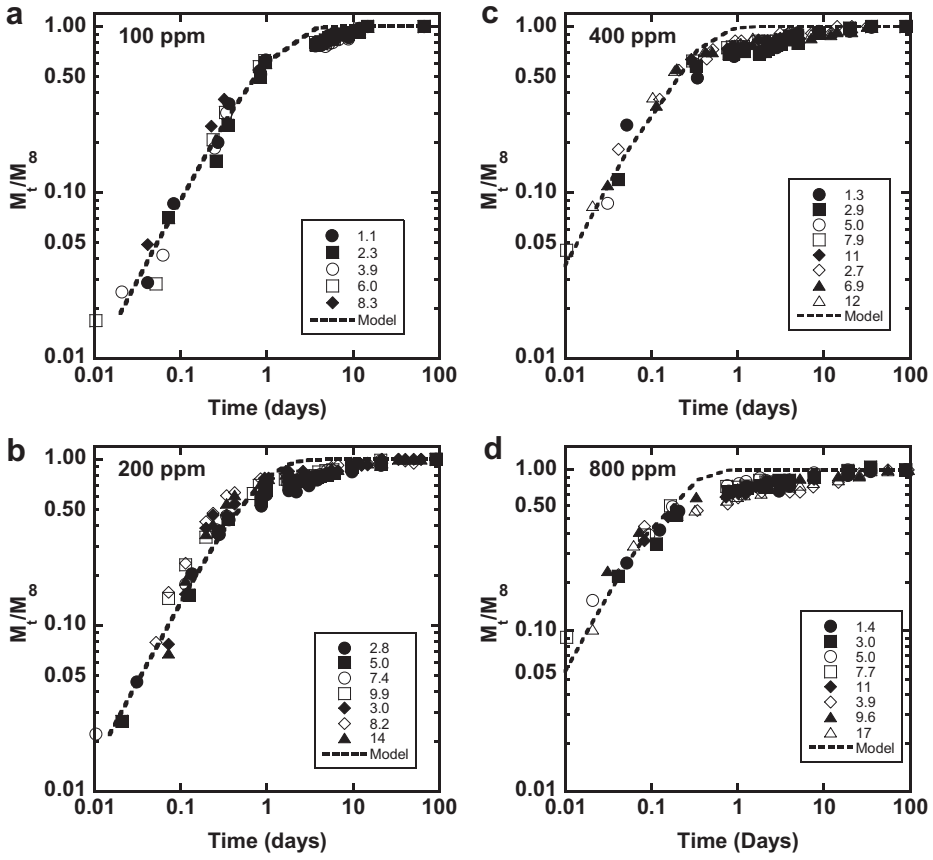

Fig. 7. Plots of thin film oxygen uptake data versus time using logarithmic coordinates for SBS films containing (a) 100 ppm, (b) 200 ppm, (c) 400 ppm, and (d) 800 ppm of cobalt catalyst normalized by M_∞. The dashed lines show kinetic model predictions using the average values of k_R and $\widehat{\nu}$ for each catalyst loading.

of the oxidized polymer film. In the following calculations of M_t and M_∞, the contribution of any dissolved oxygen is considered negligible.

The rate of uptake can be approximated as

$$\frac{\partial M_t}{\partial t} = \frac{2M_\infty}{L}\frac{\mathrm{d}x_f}{\mathrm{d}t} = \frac{32n_0}{\rho_{\mathrm{un}}\widehat{\nu}}\frac{2}{L}\frac{\mathrm{d}x_f}{\mathrm{d}t} \tag{13}$$

A corresponding relationship can be obtained from the molar flux from Fick's law given in Equation (12), i.e.,

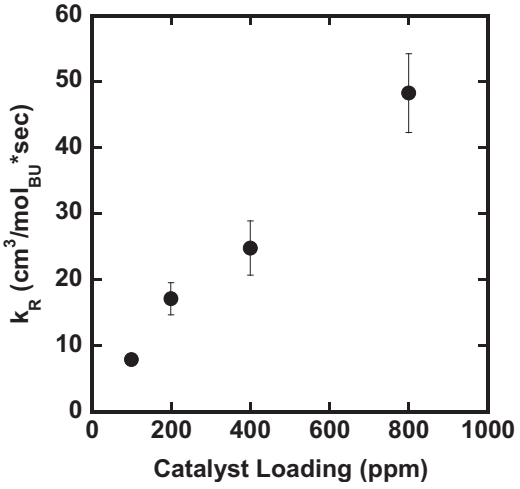

Fig. 8. Reaction rates constant k_R versus cobalt catalyst loading in SBS films.

$$\frac{\partial M_t}{\partial t} = \frac{2\times 32M_\infty}{\rho_{\mathrm{un}}L}(\text{molar O}_2\text{ flux}) = \frac{64}{\rho_{\mathrm{un}}\widehat{\nu}}\frac{D_{ox}C_0}{x_f} \tag{14}$$

Equations (13) and (14) can be equated and subsequently integrated to obtain

$$\int_{x_{f_0}}^{x_f} x_f \mathrm{d}x_f = \int_{t_0}^{t}\frac{D_{ox}\widehat{\nu}C_0}{n_0}\mathrm{d}t \tag{15}$$

Solving for x_f gives

$$x_f = \left[x_{f_0}^2 + \frac{2D_{ox}\widehat{\nu}c_0}{n_0}(t-t_0)\right]^{1/2} \tag{16}$$

The normalized oxygen uptake is then

$$\frac{M_t}{M_\infty} = \frac{2}{L}\left[x_{f_0}^2 + \frac{2D_{ox}\widehat{\nu}c_0}{n_0}(t-t_0)\right]^{1/2} \tag{17}$$

Since the model envisioned in Fig. 9 would not apply until longer times, the beginning limits of integration are not well defined. However, we might expect that

$$x_{\mathrm{fo}} = L_c \tag{18}$$

and that t_0 would be proportional to t_{ox}, as defined earlier, thus

$$t_0 \sim \frac{\alpha}{\widehat{\nu}k_R C_0} \tag{19}$$

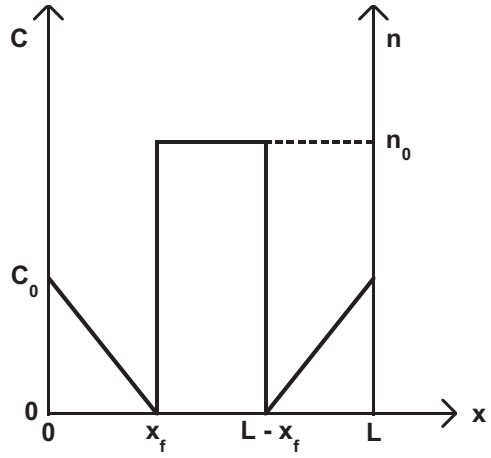

Fig. 9. Physical picture for the approximate moving-boundary model for thick film oxidation behavior at long oxidation times.

where α is a proportionality factor. The model can be written in the following general form

$$\frac{M_t}{M_\infty} = (a + bt)^{1/2} \tag{20}$$

where the values of a and b predicted by the model are as follows

$$a \sim 4\left[\left(\frac{L_c}{L}\right)^2 - \frac{2\alpha D_{ox}}{k_R n_0 L^2}\right] \tag{21}$$

and

$$b \sim \frac{8 D_{ox} \hat{\nu} C_0}{n_0 L^2} \tag{22}$$

Equation (20) can be re-expressed in the form

$$\left(\frac{M_t}{M_\infty}\right)^2 = a + bt \tag{23}$$

Fig. 10 shows an example of $(M_t/M_\infty)^2$ plotted versus oxidation times, excluding the early time data where this model is not expected to apply, for two thick films containing 200 ppm of catalyst. The experimental data of $(M_t/M_\infty)^2$ data increase linearly with time, as expected from the model for thick films. Quite similar

Table 3
Values of slopes b and intercepts a theoretically extracted from all thick film oxygen uptake data at long oxidations.

Catalyst ppm	L μm	b = Slope 10^{-8}/s	a = Intercept ND
100	134	1.20	0.110
	143	1.47	0.095
	175	1.01	0.046
	189	9.30	0.036
200	117	1.69	0.095
	166	1.08	0.084
	205	9.24	0.054
	232	3.82	0.041
	266	9.48	0.031
400	116	2.90	0.153
	137	2.54	0.135
	168	1.58	0.088
	188	1.07	0.059
	212	9.07	0.049
	272	7.24	0.042
800	95	4.20	0.105
	107	2.74	0.094
	117	2.58	0.086
	124	3.09	0.065
	141	1.57	0.088
	179	1.54	0.062
	191	1.31	0.039

plots were obtained for all thick films at each catalyst loading. From these linear plots the slopes b and intercepts a were extracted for all thick films and recorded in Table 3. In fact, plotting M_t/M_∞ versus $(a + bt)^{1/2}$ for all thick films, using values of a and b from plots like Fig. 10, makes a universal straight line with slope of unity, as shown in Fig. 11. This plot validates the form of the model and the method of extracting slopes b and intercepts a from the data. Note that Fig. 11 neglects data from the early time regime, when diffusion is fast and oxidation is kinetically controlled. As expected the short time data do not collapse into a single curve, since the current model considers an oxidation that is controlled by diffusion for films with thicknesses $L > 2L_c$.

Equations (21) and (22) predict that a and b should scale as the inverse square of film thickness. The solid points in Fig. 12 show the values of a and b determined by statistically fitting the long time data for thick films to Equations (21) and (22) plotted versus L on log–log coordinates. The solid lines in Fig. 12 are the predictions by Equations (21) and (22) using average values of L_c and $\hat{\nu}$ and assuming $\alpha \sim 0$. The data points generally lie parallel to the

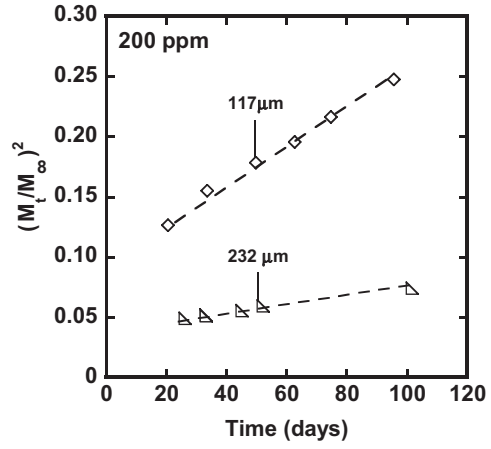

Fig. 10. Representative plots of thick film oxygen uptake versus time at long oxidation times to obtain values of slopes b and intercepts a in Equation (22), see Table 3.

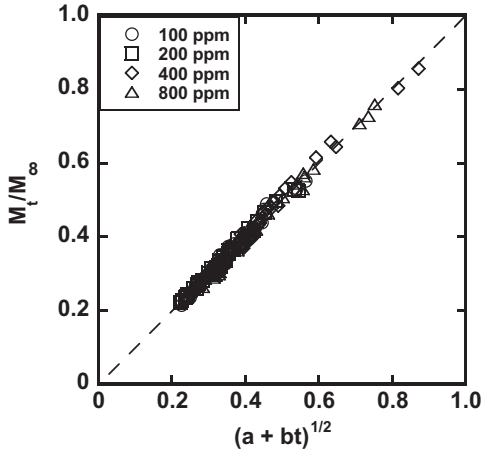

Fig. 11. Universal plot of M_t/M_∞ versus $(a + bt)^{1/2}$ for all thick films at long oxidation times. Data points for the early time regime are not included here.

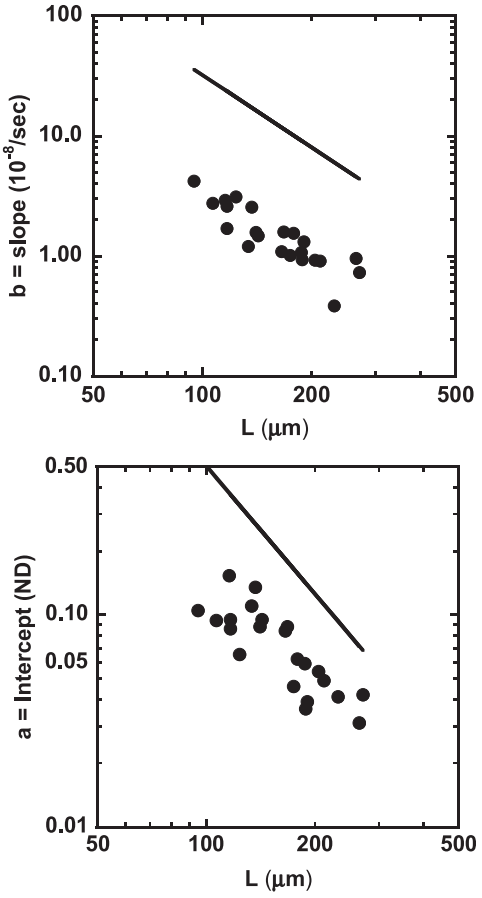

Fig. 12. Slopes b and intercepts a calculated from the data via fitting to Equation (22) plotted versus thickness L plotted on logarithmic coordinates. The data are consistent with L^{-2} dependence of both a and b as predicted by the model, i.e., the solid lines were constructed using average vales of critical thickness (L_c = 35.5 μm) and stoichiometric coefficients ($\hat{\nu}$ = 1.68 mol_{PB}/mol_{O_2}) for all catalyst loadings. The absolute values of a and b are lower than the theoretical predictions.

predicted lines, verifying the L^{-2} dependence expected, but the model over predicts both a and b. Assigning finite values to α would bring the theoretical intercepts into better agreement with the experimental values; however, the slopes would remain over predicted. Thus, the model does not quantitatively reproduce the oxygen uptake data for thick films when the measured parameters are inserted into Equations (21) and (22). At least part of this failure might have to do with the fact that the model for the early stages of oxidation in thick films where reaction kinetics controls has not been rigorously merged with the late stage where diffusion controls. Certainly there is an intermediate stage where both kinetics and diffusion must be considered. In any case, this model does appear to capture, at least qualitatively, the behavior for thick films.

4. Conclusions

A styrene-butadiene-styrene block copolymer with varying amounts of a cobalt catalyst was evaluated as an oxygen scavenging component for barrier systems. The oxygen uptake of SBS films containing four catalyst loadings and having a wide range of thicknesses was experimentally measured and analyzed by simple theories. For thin enough films, the rate of oxygen uptake is controlled by the reaction of the butadiene units with oxygen and is not affected by oxygen diffusion. A simple thin film model allowed extraction of reaction rate and stoichiometric parameters from the experimental data for the oxidation conditions considered in the current study.

At long times for thicker films, the oxygen uptake process is limited by the rate of oxygen diffusion, and a simplified moving-boundary model describes this region semi-quantitatively. The division between the two regimes can be understood in terms of the concept of a "critical thickness L_c" introduced in earlier papers. For films with thickness $L \leq 2L_c$, chemical kinetics is largely the rate controlling process and such films became fully oxidized over the time scale of the current observation, ~90 days. For thicker films with thicknesses $L > 2L_c$ full oxidation was not achieved within 90 days. Values for L_c were deduced by a simple two regime analysis of the data. These values agree well with observations of cross-sectional surfaces of partially oxidized films made by SEM analysis. The outer region becomes hard and brittle while the interior retains more of the appearance of the native SBS copolymer.

The fully oxidized polymer has an oxygen permeability that is two orders of magnitude lower than the un-oxidized SBS material. This fact contributes to the trend towards diffusion control of oxygen uptake in thick films at long times. This fact may be quite beneficial when the scavenging component is incorporated into barrier films as layers by co-extrusion [14]. It should be noted, however, that the oxidized form of SBS is still 2–3 times more permeable to oxygen than the conventional barrier material poly(ethylene terephthalate) [42].

Future design and modeling of blend and laminate barrier films based on the SBS/cobalt catalyst system discussed here should benefit from the fundamental understanding of reaction kinetics and parameters deduced by the current study. A remaining need is for a theoretical model to predict the critical thickness from basic principles rather than using the extensive experimental protocols discussed here. This would be helpful in designing experiments (i.e., how thin should the films be?) for extraction of kinetic and stoichiometric data quickly and efficiently.

Acknowledgments

This research was supported by NSF Science and Technology Center for Layered Polymeric Systems (Grant DMR-0423914). Helpful experimental and modeling discussions with Richard Hua Li and Susana Carranza is gratefully acknowledged.

References

[1] Rooney ML. Active packaging in polymer films. In: Rooney ML, editor. Active food packaging. London: Blackie Academic and Professional; 1995. p. 74–110.
[2] Burrows PE. Gas permeation and lifetime tests on polymer-based barrier coatings. In: Proceedings of SPIE. SPIE; 2001. p. 75–83.
[3] Choi M-C, Kim Y, Ha C-S. Progress in Polymer Science 2008;33(6):581–630.
[4] Lewis J. Materials Today 2006;9(4):38–45.
[5] Cochran MA, Folland R, Nicholas JW, Edward M, Robinson R. Packaging, U.S.. Patent 5,639,815; 1997.
[6] Cochran MA, Folland R, Nicholas JW, Robinson R. Packaging, U.S.. Patent 5,021,515; 1991.
[7] Ferrari MC, Carranza S, Bonnecaze RT, Tung KK, Freeman BD, Paul DR. Journal of Membrane Science 2009;329(1–2):183–92.
[8] Carranza S, Paul DR, Bonnecaze RT. Journal of Membrane Science 2010; 360(1–2):1–8.
[9] Carranza S, Paul DR, Bonnecaze RT. Chemical Engineering Science 2010;65(3): 1151–8.
[10] Li H, Ashcraft DK, Freeman BD, Stewart M, Jank MK, Clark TR. Polymer 2008; 49(21):4541–5.
[11] Li H, Tung KK, Paul DR, Freeman BD, Stewart M, Jenkins J. Industrial & Engineering Chemistry Research 2012;51(21):7138–45.
[12] Li H, Tung KK, Paul DR, Freeman BD. Polymer 2011;52(13):2772–83.
[13] Carranza S. Modeling of oxygen scavenging polymers and composites (Ph.D. thesis). The University of Texas at Austin; 2010.
[14] Carranza S, Paul DR, Bonnecaze RT. Journal of Membrane Science 2012; 399–400:73–85.

[15] Adam C, Lacoste J, Lemaire J. Polymer Degradation and Stability 1989:24185–200.
[16] Bauman RG, Maron SH. Journal of Polymer Science 1956;22:1–12.
[17] Beavan SW, Phillips D. European Polymer Journal 1974;10(7):593–603.
[18] Ivanov VB, Burkova SG, Morozov YL, Shlyapintokh VY. Kinetika i Kataliz 1979; 20:51330–3.
[19] Piton M, Rivaton A. Polymer Degradation and Stability 1996;53(3):343–59.
[20] Rabek JF, Lucki J, Ranby B. European Polymer Journal 1979:151089–100.
[21] Clough RL, Gillen KT. Polymer Degradation and Stability 1992;38(1):47–56.
[22] Wise J, Gillen KT, Clough RL. Polymer 1997;38(8):1929–44.
[23] Coquillat M, Verdu J, Colin X, Audouin L, Nevière R. Polymer Degradation and Stability 2007;92(7):1326–33.
[24] Coquillat M, Verdu J, Colin X, Audouin L, Nevière R. Polymer Degradation and Stability 2007;92(7):1334–42.
[25] Coquillat M, Verdu J, Colin X, Audouin L, Nevière R. Polymer Degradation and Stability 2007;92(7):1343–9.
[26] Gillen KT, Clough RL. Polymer 1992;33(20):4358–65.
[27] Rincon-Rubio LM, Fayolle B, Audouin L, Verdu J. Polymer Degradation and Stability 2001;74(1):177–88.
[28] Bigger SW, Delatycki O. Journal of Polymer Science, Part A: Polymer Chemistry 1987;25(12):3311–23.
[29] Lissi EA, Encinas MV. Photoinitiators for free radical polymerization. In: Rabek JF, editor. Photochemistry and photophysics. Boca Raton: CRC Press; 1991.
[30] Adam C, Lacoste J, Lemaire J. Polymer Degradation and Stability 1989;26(3): 269–84.
[31] Katsumoto K, Ching TY, Goodrich JL, Speer DV. Photoinitiators and oxygen scavenging composition, U.S. patent 6,139,770; 2000.
[32] Adam C, Lacoste J, Lemaire J. Polymer Degradation and Stability 1990;29(3): 305–20.
[33] Sheldon RA, Kochi JK. Metal catalysis in peroxide reactions. In: Metal-catalyzed oxidation of organic compounds. New York: Academic Press; 1981. p. 38–48.
[34] Koros WJ, Paul DR. Journal of Polymer Science: Polymer Physics Edition 1976; 14(10):1903–7.
[35] Kim J, Kim P, Lee H. Journal of Applied Polymer Science 1997;66(6): 1117–22.
[36] Song KW, Ka KR, Kim CK. Industrial & Engineering Chemistry Research 2010; 49(14):6587–92.
[37] Van Amerongen GJ. Journal of Polymer Science 1950;5(3):307–32.
[38] Massey Liesl K. Permeability properties of plastics and elastomers - a guide to packaging and barrier materials. 2nd ed. William Andrew Publishing/Plastics Design Library; 2003.
[39] Sperling LH. Introduction to Physical Polymer Science. 2nd ed. New York: Wiley; 1992.
[40] Lee WM. Polymer Engineering and Science 1980;20(1):65–9.
[41] Paul DR. Fundamentals of transport phenomena in polymer membranes. In: Drioli Enrico, Giorno Lidietta, editors. Comprehensive membrane science and engineering. 1st ed. Elsevier B.V.; 2010. p. 75–90.
[42] Andrade GS, Collard DM, Schiraldi DA, Hu Y, Baer E, Hiltner A. Journal of Applied Polymer Science 2003;89(4):934–42.